

# Order $m\alpha^6$ contributions to ground-state hyperfine splitting in positronium

G. S. Adkins

*Franklin and Marshall College, Lancaster, Pennsylvania 17604*

J. Sapirstein

*Department of Physics, University of Notre Dame, Notre Dame, Indiana 46556*

(Received 8 April 1998)

A Bethe-Salpeter based bound-state formalism is applied to the calculation of recoil contributions of order  $m\alpha^6$  to hyperfine splitting in ground-state positronium. The calculation involves the numerical evaluation of two- and three-photon exchange diagrams along with derivative terms and many-potential contributions. After inclusion of all other contributions of the same order, a comparison with other calculations and experiment is made. [S1050-2947(98)02911-4]

PACS number(s): 36.10.Dr, 12.20.Ds, 31.15.Md, 31.30.Jv

## INTRODUCTION

Because of the equality of the masses of the electron and positron and their pointlike nature, there exists only one expansion parameter for positronium, the fine-structure constant  $\alpha$ . Corrections to the basic energy scale of a rydberg are thus given as  $\alpha^r$  Ry. Calculations of the  $r=2$  term were made by Pirenne [1] and Beretstetski and Landau [2] and completed by Ferrell [3]. A few years after the development of the modern form of quantum electrodynamics (QED), Fulton and Martin [4] calculated the leading QED corrections with  $r=3$ . While logarithmic terms of the next higher order were calculated for hyperfine structure in the 1970s [5] and for fine structure in the early 1990s [6], it is a remarkable fact that it has taken more than 40 years for the complete calculation of constant terms of order  $r=4$  to be completed. Very recently, however, this has been achieved through the calculation of three separate effects. The first is the evaluation of two-loop radiative corrections to one-photon annihilation [7,8]. In Ref. [7] the calculation is carried out with Bethe-Salpeter based techniques and is specific to ground-state hyperfine splitting, the energy difference between the triplet ( $1^3S_1$ ) and singlet ( $1^1S_0$ ) states. It is in excellent agreement with the result of Ref. [8], which is carried out in the framework of nonrelativistic QED (NRQED) [9], and is valid for all states. The second is the evaluation by Pachucki [10], in an effective Hamiltonian approach, similar to NRQED, of recoil contributions of order  $m\alpha^6$ . However, in this case there is a significant disagreement with a previous NRQED calculation [9] for hyperfine splitting. Finally, radiative recoil effects, which previously had been calculated only for ground-state hyperfine splitting [11], have been extended to all states by Pachucki and Karshenboim [12].

In this paper we present a calculation of recoil corrections to positronium hyperfine splitting of order  $m\alpha^6$ . The calculation involves the evaluation of derivative terms, many-potential terms, two-photon exchange diagrams, and three-photon exchange diagrams. While this same calculation was carried out for arbitrary states by Pachucki [10] in his effective Hamiltonian formalism, here we specialize to the ground state, using the same Bethe-Salpeter formalism as that used in Ref. [7]. However, while the use of this formalism led to

very good agreement with NRQED for two-loop radiative corrections [7,8], in this case the agreement with NRQED is poor: Specifically, our result of 1.32(7) MHz is almost three standard deviations away from the Caswell-Lepage result of 3.12(0.66) MHz. An even stronger disagreement exists with the 7.03(3)-MHz result of Pachucki.

The plan of the paper is as follows. In Sec. I we first briefly describe the bound-state formalism used. While the full calculation has been carried out only for ground-state hyperfine splitting, we present the energy shifts associated with certain parts of the calculation, specifically derivative terms, many-potential terms, and one-photon exchange, for both the ground-state hyperfine interval and the singlet state, which is of course equivalent to evaluating the singlet and triplet separately. We then specialize to hyperfine splitting for the remainder of the calculation, which involves the evaluation of two- and three-photon exchange diagrams. This is a simpler calculation than calculating the singlet and triplet separately, as a set of infrared sensitive effects connected with the Bethe logarithm cancel out. While we will not present final results for the singlet, we discuss certain complications concerning the relation of the Bethe logarithm to the formalism in Sec. II. Finally, the present status of theory and experiment is treated in Sec. III.

## I. FORMALISM

Because the Bethe-Salpeter method we use is a relatively standard one, being a modification of that presented by Caswell and Lepage [13], we describe it only briefly. The first element of the formalism is the choice of propagator

$$S_0(p) = -\frac{2\pi i \delta(p_0)}{2\omega_p - E} [\Lambda_+(\vec{p}) \gamma^0]^{(1)} [\Lambda_-(\vec{p}) (-\gamma^0)]^{(2)T}. \quad (1)$$

Here  $\omega_p = \sqrt{\vec{p}^2 + m^2}$ ,  $E$  is the total energy in the center of mass, and the projection operators are given by

$$\Lambda_{\pm}(\vec{p}) = \frac{1}{2\omega_p} [\omega_p \pm (m - \vec{\gamma} \cdot \vec{p}) \gamma^0]. \quad (2)$$

The lowest-order problem is defined in terms of the kernel

$$K_0(p', p) = \left( \frac{2\omega_{p'}}{\omega_{p'} + m} \right) \left( \frac{2m}{\omega_{p'} + W} \right)^{1/2} (-i)V(\vec{p}' - \vec{p}) \\ \times \left( \frac{2m}{\omega_p + W} \right)^{1/2} \left( \frac{2\omega_p}{\omega_p + m} \right) \left[ \frac{1 + \gamma^0}{2} \right]^{(1)} \left[ \frac{1 - \gamma^0}{2} \right]^{(2)T}. \quad (3)$$

Here  $W = E/2$  and  $V(\vec{p}' - \vec{p})$  is the Coulomb potential,

$$V(\vec{p}' - \vec{p}) = - \frac{4\pi\alpha}{|\vec{p}' - \vec{p}|^2}. \quad (4)$$

The factors involving  $1 + \gamma^0$  and  $1 - \gamma_0$ , which are close to unity for the electron and positron, respectively, in the non-relativistic limit, play an important role in numerator simplification when they surround Dirac propagators and together with the other factors in the kernel turn the set of ladder diagrams with Dirac propagators into the nonrelativistic Coulomb Green's function. With the above propagator and kernel, the ground-state wave function for the singlet is

$$\psi(p) = 2\pi\delta(p_0) \frac{1}{\sqrt{8}} \phi(\vec{p}) \frac{1}{2\omega_p(\omega_p + m)} \sqrt{\frac{W_0 + \omega_p}{2W_0}} \\ \times (\not{p} + m)(1 + \gamma^0)\gamma_5(\not{p} - m)\gamma_0, \quad (5)$$

with

$$\phi(\vec{p}) = \frac{8\pi\gamma}{(\vec{p}^2 + \gamma^2)^2} \left( \frac{\gamma^3}{\pi} \right)^{1/2}, \quad (6)$$

where  $\gamma = m\alpha/2$  and  $W_0 = \sqrt{1 - \gamma^2}$ . The triplet state differs from the singlet only in the replacement  $\gamma_5 \rightarrow \not{\epsilon}$ , where  $\epsilon = (0, \vec{\epsilon})$  is the spin vector of the triplet state. More details of the procedure are given by Adkins and Fell [14].

Once this formalism has been chosen, perturbation theory in the perturbing kernel  $\delta K \equiv K - K_0$ , with  $K$  the complete kernel, can be applied in a straightforward manner. The calculation divides into three parts: a derivative term, a many-potential term, and two-photon and three-photon exchange diagrams.

The simplest part of the calculation is the derivative term, whose leading term is given formally by  $(\delta K)(\delta K)'$ . The first term, neglecting annihilation kernels, which have been treated elsewhere, is simply the leading fine structure  $\frac{1}{3}m\alpha^4$  for hyperfine splitting and  $-\frac{3}{8}m\alpha^4$  for the singlet. The second term vanishes for single Coulomb and transverse photon exchange, as they do not depend on the total energy (higher-order kernels do have energy dependence, but contribute to orders beyond  $m\alpha^6$ ), but  $K_0$  does have energy dependence, which leads to the energy shifts

$$\Delta E_d^{\text{hfs}} = - \frac{1}{24} m\alpha^6 \quad (7)$$

for hyperfine splitting and

$$\Delta E_d^{\text{singlet}} = \frac{3}{64} m\alpha^6 \quad (8)$$

for the singlet.

The many-potential term arises from the formal form  $\delta KG\delta K$ , which comes from standard second-order Rayleigh-Schrödinger perturbation theory. In the present formalism, the reference Green's function is directly proportional to the nonrelativistic Coulomb Green's function, which in momentum space breaks up naturally into a free propagator, a one potential part in which free propagators occur before and after a single interaction with the Coulomb potential, and a many potential part in which two or more Coulomb interactions take place. The first two terms are combined with the two- and three-photon diagrams discussed below, leaving only the many-potential term  $\delta KG_{\text{MP}}\delta K$ . Again leaving out the annihilation kernel, the only kernels that contribute to the order of interest are the difference of Coulomb photon exchange with the reference kernel, which we designate as  $\delta K_0$ , and transverse photon exchange, designated  $T$ . We then consider the combinations  $\delta K_0 \cdot \delta K_0$ ,  $\delta K_0 \cdot T$ ,  $T \cdot \delta K_0$ , and  $T \cdot T$ . The first gives no contribution to the hyperfine splitting and contributes

$$\Delta E_{\text{MP}}^{\text{singlet}}(\delta K_0 \cdot \delta K_0) = 0.000\,446m\alpha^6 \quad (9)$$

to the singlet. The second and third, which are equal to one another, sum to

$$\Delta E_{\text{MP}}^{\text{hfs}}(\delta K_0 \cdot T + T \cdot \delta K_0) = 0.053\,745m\alpha^6 \quad (10)$$

for hyperfine splitting and

$$\Delta E_{\text{MP}}^{\text{singlet}}(\delta K_0 \cdot T + T \cdot \delta K_0) = -0.052\,937m\alpha^6 \quad (11)$$

for the singlet. Finally, the  $T - T$  contribution is

$$\Delta E_{\text{MP}}^{\text{hfs}}(T \cdot T) = 0.367\,198m\alpha^6 \quad (12)$$

for hyperfine splitting and

$$\Delta E_{\text{MP}}^{\text{singlet}}(T \cdot T) = -0.373\,518m\alpha^6 \quad (13)$$

for the singlet. We note that the result of Eq. (10) differs from the result found by Caswell and Lepage, as expected because of the different formalism used, but Eq. (12), which is less sensitive to the formalism, is in agreement with them.

The main part of the calculation is associated with the evaluation of two- and three-photon exchange diagrams. While the connection with the bound-state formalism is somewhat complex, it is straightforward to write down the general form of the diagrams we consider. We represent the photon propagator in Coulomb gauge as  $D_{\mu\nu}^C(q)$ , where

$$D_{00}^C(q) = \frac{1}{q^2}, \quad (14)$$

$$D_{0i}^C(q) = D_{i0}^C(q) = 0,$$

$$D_{ij}^C(q) = \frac{1}{q^2 + i\epsilon} \left( \delta_{ij} - \frac{q_i q_j}{q^2} \right).$$

We now introduce the three kinds of diagrams that can contribute to hyperfine splitting in order  $m\alpha^6$ , namely, one-photon, two-photon, and three-photon exchange diagrams. One-photon exchange (in the absence of radiative corrections) is given by

$$\Delta E_{1\gamma} = e^2 \int \frac{d^4 p'}{(2\pi)^4} \int \frac{d^4 p}{(2\pi)^4} D_{\mu\nu}^C(p'-p) \times \text{Tr}[\bar{\psi}(p') \gamma^\mu \psi(p) \gamma^\nu]. \quad (15)$$

Separating this into Coulomb and transverse photon contributions, these contribute

$$\Delta E_C^{\text{hfs}} = m\alpha^6 \left[ -\frac{1}{48} \ln \alpha - 0.019\,217 \right] \quad (16)$$

and

$$\Delta E_T^{\text{hfs}} = \frac{1}{3} m\alpha^4 - \frac{1}{2} m\alpha^5 + m\alpha^6 \left[ -\frac{1}{6} \ln \alpha + 0.360\,801 \right] \quad (17)$$

for hyperfine splitting and

$$\Delta E_C^{\text{singlet}} = -\frac{1}{2} m\alpha^2 - \frac{1}{8} m\alpha^5 + m\alpha^6 \left[ -\frac{7}{128} \ln \alpha + 0.085\,004 \right] \quad (18)$$

and

$$\Delta E_T^{\text{singlet}} = -\frac{3}{8} m\alpha^4 + \frac{3}{8} m\alpha^5 + m\alpha^6 \left[ -\frac{1}{16} \ln \alpha - 0.379\,234 \right] \quad (19)$$

for the singlet energy.

There are two topologies for two photon exchange: uncrossed

$$\Delta E_{2\gamma 0} = ie^4 \int \frac{d^4 k}{(2\pi)^4} \int \frac{d^4 p'}{(2\pi)^4} \int \frac{d^4 p}{(2\pi)^4} \times D_{\mu\rho}^C(p'-k) D_{\nu\lambda}^C(k-p) \times \text{Tr} \left[ \bar{\psi}(p') \gamma^\mu \frac{1}{\not{P}/2 + \not{k} - m + i\epsilon} \gamma^\nu \psi(p) \times \gamma^\lambda \frac{1}{-\not{P}/2 + \not{k} - m + i\epsilon} \gamma^\rho \right] \quad (20)$$

and crossed

$$\Delta E_{2\gamma X} = ie^4 \int \frac{d^4 k}{(2\pi)^4} \int \frac{d^4 p'}{(2\pi)^4} \int \frac{d^4 p}{(2\pi)^4} \times D_{\mu\rho}^C(p'-k) D_{\nu\lambda}^C(k-p) \times \text{Tr} \left[ \bar{\psi}(p') \gamma^\mu \frac{1}{\not{P}/2 + \not{k} - m + i\epsilon} \times \gamma^\nu \psi(p) \gamma^\rho \frac{1}{-\not{P}/2 - \not{k} + \not{p} + \not{p}' - m + i\epsilon} \gamma^\lambda \right]. \quad (21)$$

Finally, there are six topologies for three-photon exchange, of which four are independent. The first we refer to as the ‘‘0’’ class, which has the topology of a three-rung ladder,

$$\Delta E_{3\gamma 0} = -e^6 \int \frac{d^4 k}{(2\pi)^4} \int \frac{d^4 l}{(2\pi)^4} \int \frac{d^4 p'}{(2\pi)^4} \int \frac{d^4 p}{(2\pi)^4} \times D_{\mu\rho}^C(p'-l) D_{\nu\lambda}^C(l-k) D_{\alpha\beta}^C(k-p) \times \text{Tr} \left[ \bar{\psi}(p') \gamma^\mu \frac{1}{\not{P}/2 + \not{l} - m + i\epsilon} \times \gamma^\nu \frac{1}{\not{P}/2 + \not{k} - m + i\epsilon} \gamma^\alpha \psi(p) \times \gamma^\beta \frac{1}{-\not{P}/2 + \not{k} - m + i\epsilon} \gamma^\lambda \frac{1}{-\not{P}/2 + \not{l} - m + i\epsilon} \gamma^\rho \right]. \quad (22)$$

The next two, which we refer to as the ‘‘Y’’ class, are equal, so we evaluate only one explicitly, accounting for the other by doubling, giving

$$\Delta E_{3\gamma Y} = -2e^6 \int \frac{d^4 k}{(2\pi)^4} \int \frac{d^4 l}{(2\pi)^4} \int \frac{d^4 p'}{(2\pi)^4} \int \frac{d^4 p}{(2\pi)^4} \times D_{\mu\rho}^C(p'-l) D_{\nu\lambda}^C(l-k) D_{\alpha\beta}^C(k-p) \times \text{Tr} \left[ \bar{\psi}(p') \gamma^\mu \frac{1}{\not{P}/2 + \not{l} - m + i\epsilon} \gamma^\nu \frac{1}{\not{P}/2 + \not{k} - m + i\epsilon} \times \gamma^\alpha \psi(p) \gamma^\lambda \frac{1}{-\not{P}/2 + \not{l} - \not{k} + \not{p} - m + i\epsilon} \times \gamma^\beta \frac{1}{-\not{P}/2 + \not{l} - m + i\epsilon} \gamma^\rho \right]. \quad (23)$$

Similar remarks apply to the next two contributions, referred to as the ‘‘Z’’ class, which are

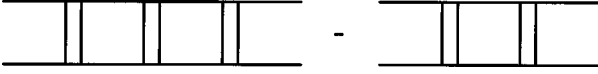


FIG. 1. Bethe-Salpeter perturbation scheme: Double lines represent irreducible kernels.

$$\begin{aligned} \Delta E_{3\gamma Z} = & -2e^6 \int \frac{d^4 k}{(2\pi)^4} \int \frac{d^4 l}{(2\pi)^4} \int \frac{d^4 p'}{(2\pi)^4} \int \frac{d^4 p}{(2\pi)^4} \\ & \times D_{\mu\rho}^C(p'-l) D_{\nu\lambda}^C(l-k) D_{\alpha\beta}^C(k-p) \\ & \times \text{Tr} \left[ \bar{\psi}(p') \gamma^\mu \frac{1}{\not{P}/2 + \not{l} - m + i\epsilon} \gamma^\nu \frac{1}{\not{P}/2 + \not{k} - m + i\epsilon} \right. \\ & \times \gamma^\alpha \psi(p) \gamma^\lambda \frac{1}{-\not{P}/2 + \not{l} - \not{k} + \not{p} - m + i\epsilon} \\ & \left. \times \gamma^\rho \frac{1}{-\not{P}/2 - \not{k} + \not{p} + \not{p}' - m + i\epsilon} \gamma^\beta \right]. \quad (24) \end{aligned}$$

Finally, when all photons are crossed we define the contribution to be an ‘‘X’’ diagram, given by

$$\begin{aligned} \Delta E_{3\gamma X} = & -e^6 \int \frac{d^4 k}{(2\pi)^4} \int \frac{d^4 l}{(2\pi)^4} \int \frac{d^4 p'}{(2\pi)^4} \int \frac{d^4 p}{(2\pi)^4} \\ & \times D_{\mu\rho}^C(p'-l) D_{\nu\lambda}^C(l-k) D_{\alpha\beta}^C(k-p) \\ & \times \text{Tr} \left[ \bar{\psi}(p') \gamma^\mu \frac{1}{\not{P}/2 + \not{l} - m + i\epsilon} \right. \\ & \times \gamma^\nu \frac{1}{\not{P}/2 + \not{k} - m + i\epsilon} \gamma^\alpha \psi(p) \\ & \times \gamma^\rho \frac{1}{-\not{P}/2 - \not{l} + \not{p} + \not{p}' - m + i\epsilon} \\ & \left. \times \gamma^\lambda \frac{1}{-\not{P}/2 - \not{k} + \not{p} + \not{p}' - m + i\epsilon} \gamma^\beta \right]. \quad (25) \end{aligned}$$

While we are interested in contributions of order  $m\alpha^6$ , some of the above diagrams can contribute to lower orders when Coulomb photons are adjacent to wave functions and we wish to isolate such terms. This is done automatically by the bound-state formalism. The contribution to energy shifts can be represented very compactly by Fig. 1, which is closely related to the form derived and used by Caswell and Lepage in Ref. [13]. The solid vertical bars represent all irreducible kernels, which for the present calculation can be limited to the kernels shown in Fig. 2. Different kernels require rather different treatment, so we now analyze them one at a time. The basic strategy that is used in the following is,

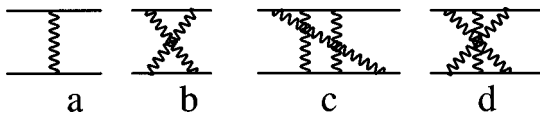


FIG. 2. Irreducible kernels entering the present calculation.



FIG. 3.  $Y$ -class diagrams: The transverse photon diagram (a) requires no corrections, but the Coulomb photon diagram (b) requires a formalism-dependent subtraction.

whenever a single Coulomb photon is exchanged to the rightmost of a diagram, to make the rearrangement  $SC = (SC - S_0 K_0) + S_0 K_0 \equiv R + S_0 K_0$ , where  $S$  is the propagator immediately to the left of the Coulomb photon  $C$  and  $S_0$  and  $K_0$  were defined above. Similarly, we can also write  $CS = (CS - K_0 S_0) + K_0 S_0 \equiv \bar{R} + K_0 S_0$ . One then exploits the fact that the first part of the breakup,  $R$  or  $\bar{R}$ , is small, which frequently allows the neglect of that term, after which the remaining part can be absorbed into the wave function, which satisfies the equations  $S_0 K_0 \psi = \psi$  and  $\bar{\psi} K_0 S_0 = \bar{\psi}$ . We will see in Sec. II, however, that if highly nonrelativistic momentum regions are important, as they are for the singlet and triplet states separately, terms involving  $R$  and  $\bar{R}$  must be treated with particular care, as they can contribute in situations in which the hyperfine calculation allows them to be neglected.

We first discuss the kernels of Figs. 2(c) and 2(d), which are the only irreducible three-photon kernels. Figure 2(c) is the diagrammatic representation of the  $Z$  class defined by Eq. (24) and Fig. 2(d) is that of the  $X$  class defined by Eq. (25). In terms of Fig. 1, if these are used as any of the solid bars, the remaining kernels must be single-Coulomb-photon exchange, as any other kernel would contribute in a higher order. These photons can be absorbed into the wave function after making the rearrangement introduced above, with the net result that the diagram with three kernels becomes equal to three times the expectation value of the kernels of Figs. 2(c) and 2(d), which is canceled down to a factor of one by the diagram with two kernels. Thus no modification of Eqs. (24) and (25) is required.

Continuing to diagrams that contain the kernel of Fig. 2(b), we note that if they are accompanied by a transverse photon, there are four ways of getting a contribution of the order of interest from the three-kernel diagram (schematically, if  $X$  represents Fig. 2(b),  $XTC$ ,  $TXC$ ,  $CXT$ , and  $CTX$ ) and two from the two-kernel diagram ( $XT$  and  $TX$ ). This then leads to Eq. (23) with the photon with momentum  $p' - l$  understood to be a transverse photon, as indicated in Fig. 3(a). This is represented diagrammatically in Fig. 3(a).

Matters become more complicated when the kernel of Fig. 2(b) is accompanied by Coulomb photons. Using the breakup discussed above, it is straightforward to show that the three-kernel diagrams with Fig. 2(b) to the leftmost or rightmost, with the other kernels single Coulomb exchange, cancel the corresponding two-kernel diagrams to the order of interest. The remaining term with Fig. 2(b) in the center and single Coulomb exchanges on the sides, after making the rearrangement introduced above, becomes, when both factors of  $S_0 K_0$  are present, precisely equal to Eq. (21), which means that term can be evaluated without modification. When one  $R$  factor is present, however, the diagram contributes to the order of interest, which means that Eq. (23) is

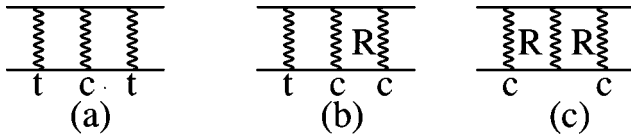


FIG. 4. 0-class diagrams: (a) requires no corrections, but (b) requires a single subtraction and (c) a double subtraction. The internal photon in (c) can be either Coulomb or transverse.

modified when the photon with momentum  $p' - l$  is a Coulomb photon by the subtraction of a similar form with the Coulomb photon replaced by  $K_0$  and the adjacent propagator by the reference propagator. The diagram representing this is given in Fig. 3(b).

The most complicated situation occurs when all kernels are one-photon exchange. If the outer photons in the first term of Fig. 1 are both transverse, then there are no terms of lower order in  $\alpha$  regardless of the nature of the inner photon and one can directly evaluate Eq. (22), as depicted in Fig. 4(a). If two photons are transverse but one photon on either side is Coulomb, our rearrangement gives a factor of 2 times the second term in Fig. 1 with two transverse photons, which leads to a factor of unity multiplying Eq. (20) with two transverse photons. If the leftmost or rightmost photon in the first term of Fig. 1 is transverse and the others Coulomb, applying our rearrangement gives a term of the form  $TCR + \tilde{R}CT$ , which is represented in Fig. 4(b), plus terms that cancel the second part of Fig. 1 with one Coulomb and one transverse photon. However, when the transverse photon is in the center, the rearrangement is of the form  $(\tilde{R} + K_0 S_0)T(R + S_0 K_0)$ , which reduces to  $\tilde{R}TR$  and  $TR + \tilde{R}T + T$ . The latter term can be rearranged into the form  $TSC + CST - T$ , which is the form we found most convenient for numerical evaluation. Finally, when all photons are Coulomb, similar arguments show that the net result is that the 0 diagram becomes  $\tilde{R}CR$ , indicated in Fig. 4(c), and a one-loop diagram of the form  $CSC - C$  is introduced. The diagrams representing the net effect of one-photon and two-photon exchange are collected together in Fig. 5.

The net result of these manipulations is that we can deal with subtracted forms of the three-photon and two-photon expressions given above. The subtraction for the two-photon expressions is particularly straightforward, as it simply involves subtracting the easily evaluated one-photon exchange terms. The three-photon expressions have modifications only for the 0 and  $Y$  classes and even for them only when a Coulomb photon is next to a wave function. The graphical representation of what is actually evaluated has been given in Figs. 2(c), 2(d), 3, and 4, which represent the three-photon exchange classes of diagrams  $Z$ ,  $X$ ,  $Y$ , and 0, and Fig. 5, which gives the two-photon exchange diagrams. When we tabulate results for the three-photon exchange diagrams, we break diagrams with unlabeled photons according to whether they are transverse ( $t$ ) or Coulomb ( $c$ ). We follow the labeling convention of following the photon lines attached to the bottom fermion line from left to right, so, for example, a  $Y$  diagram in which the first such photon is Coulomb, the second transverse, and the third again Coulomb is designated  $ctcy$ .

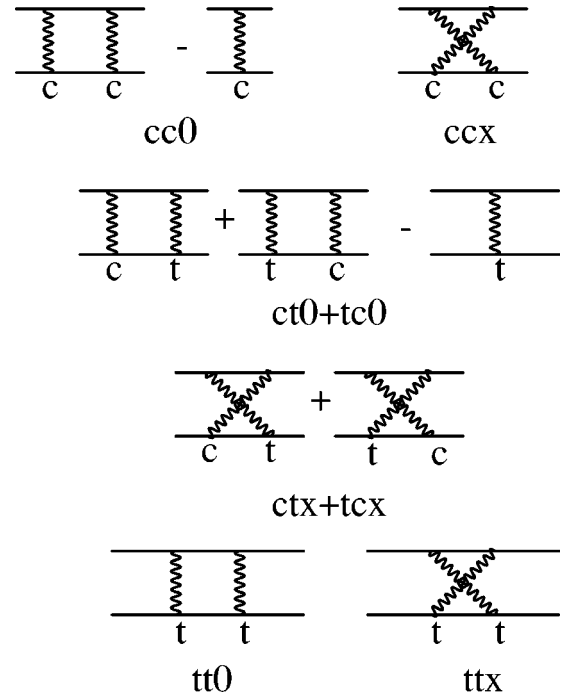


FIG. 5. Diagrams treated in Table I.

After all necessary subtractions have been implemented, we are ready to carry out the numerical evaluation of these diagrams, which is done as follows. The integrations over the fourth component of the loop momenta  $k_0$  and  $l_0$  are carried out with Cauchy's theorem. If there were poles associated with  $p_0$  and  $p'_0$ , as is the case with the Barbieri-Remiddi formalism [15], this would be a significant complication, but the factors  $\delta(p_0)$  and  $\delta(p'_0)$  in the present formalism avoid this. Even so, a large number of terms result, particularly for diagrams with three transverse photons, which break into up to 15 or 16 parts after the application of Cauchy's theorem. There then remains either a six- or a nine-dimensional integration over the spatial momenta, which is carried out with the adaptive multidimensional integration program VEGAS [16]. Whenever possible, the momenta  $p$  and  $p'$  were set equal to zero everywhere except in the wave functions. This leads to a decoupling of the integrations, with the wave function at the origin squared multiplying a simpler integral. However, this could not always be done when terms of order  $m\alpha^6 \ln \alpha$  were present. In those cases we carried out an extrapolation to  $\alpha=0$ , typically evaluating the diagrams at physical  $\alpha$ ,  $\alpha/2$ , and  $\alpha/4$  and then fitting to the form  $m\alpha^6(A + B \ln \alpha)$ . Our largest numerical errors were associated with this procedure.

We now present the results for ground-state hyperfine splitting for the two- and three-photon exchange diagrams. Starting with the two-photon exchange diagrams, we note that they contribute first in order  $m\alpha^4$ , giving  $m\alpha^4/3$ , which we do not explicitly include in Table I. We do tabulate, however, the breakdown by diagram of the known [17]  $m\alpha^5$  terms,

$$\Delta E = -\frac{m\alpha^5}{2\pi}, \quad (26)$$

along with the  $m\alpha^6$  terms of present interest.

TABLE I. Order  $m\alpha^5$  and  $m\alpha^6$  contributions to the hyperfine splitting from one-loop diagrams.

Diagram	$m\alpha^5 \ln \alpha$	$m\alpha^5$	$m\alpha^6 \ln \alpha$	$m\alpha^6$
$cc0$	0	0	$-\frac{1}{48}$	-0.0151
$ccx$	0	0	0	-0.0176
$ct0+tc0$	$\frac{2}{3\pi}$	$\frac{2 \ln 2 - 4}{3\pi}$	$\frac{1}{12}$	0.3865(12)
$ctx+tcx$	$-\frac{2}{3\pi}$	$\frac{-2 \ln 2 + 2}{3\pi}$	$\frac{1}{3}$	0.2451(5)
$tt0$	$-\frac{1}{6\pi}$	$\frac{-4 \ln 2 + 1}{18\pi}$	$-\frac{5}{24}$	-0.0598(16)
$ttx$	$\frac{1}{6\pi}$	$\frac{4 \ln 2 + 2}{18\pi}$	$-\frac{1}{6}$	-0.5618(22)

Logarithmic terms in order  $m\alpha^5$  are seen to be present in individual diagrams, but cancel in the sum. A notable feature of this part of the calculation is the difficulty of the numerical analysis, which is reflected in the relatively large numerical errors. This is in some measure the price one pays for the advantage of using a completely numerical approach: a very lengthy analysis is required, when working analytically, even for the calculation of the logarithmic terms in order  $m\alpha^6$  [18]. In the present calculation the logarithmic terms and associated constants are automatically included, but are difficult to numerically separate from the lower-order contributions. The sum of the logarithmic terms associated with two transverse photon exchange is in agreement with Fig. 4(e) of Ref. [19], but other logarithmic terms differ because of the different formalisms used.

Turning to the three-photon exchange calculation, we tabulate in Table II the individual contributions from the various diagrams. In this case, although nine-dimensional integrals had to be evaluated, there were no terms of order  $m\alpha^5$  present and the principal numerical difficulty was associated with separating out the logarithmic terms. Again comparing the latter terms with the analysis of Lepage [19], we first note that the logarithmic term in  $tct0$  is in agreement with his analysis [Fig. 4(f)], though other logarithmic terms are again formalism dependent. The sum  $-1/6m\alpha^6 \ln \alpha$  is in agreement with the known result.

We also note a cancellation of several of these terms, notably that between  $tccz$  and  $ctcy+ccty$ ,  $ctt0+ttc0$  and  $ctty$ , and  $cttx+ttcx$  and  $cttz$ . This pattern of cancellations was noted in Fig. 8 of Ref. [19]. Associated with this cancellation we note significant cancellation of constant terms. By combining the contributions together and manifesting the cancellation directly, better numerical control of the sum was obtained [20] and the results of that procedure were used in obtaining our final answer for the contribution of Table II. Including the results of Tables I and II with the derivative and many-potential terms (see Table III), we find

$$E_{3\gamma} = \left[ -\frac{1}{6} \ln \alpha + 0.0705(35) \right] m\alpha^6. \quad (27)$$

This is our principal result. Before discussing its implications

TABLE II. Order  $m\alpha^6$  contributions to hyperfine splitting from two-loop diagrams.

Graph	$m\alpha^6 \ln \alpha$	$m\alpha^6$
$tft0$	0	0.0694
$tct0$	$-\frac{5}{48}$	-0.0996
$ctt0+ttc0$	$\frac{1}{24}$	0.0163(11)
$ctc0$	$-\frac{1}{6}$	-0.2955(11)
$ctt0+tcc0$	$\frac{1}{12}$	0.1287(3)
$ccc0$	0	0.0003
$cccx$	0	-0.0039
$ctcx$	0	0.0043
$cttx+ttcx$	0	-0.0489
$tctx$	0	-0.0230
$cttx+ttcx$	$\frac{1}{24}$	0.0239
$tttx$	0	0.0041
$ttty$	0	-0.0011
$tcty+ttcy$	0	0.0558
$tccy$	0	-0.0681
$cccy$	0	-0.0010
$ctty$	$-\frac{1}{24}$	-0.1435(12)
$ctcy+ccty$	$\frac{1}{3}$	0.5317(37)
$cccz$	0	0.0063
$ctcz+cctz$	0	0.0283
$tccz$	$-\frac{1}{3}$	-0.4780(38)
$ttcz+ttcz$	0	0.0534
$cttz$	$-\frac{1}{24}$	-0.0448
$tttz$	0	-0.0011

for experiment and comparison with other calculations, we now briefly discuss some issues connected with the singlet energy.

## II. SINGLET ENERGY

A significant complication of calculating either the singlet or triplet energy by itself is the presence of  $m\alpha^5$  terms associated with the Bethe logarithm that cancel only when the difference is considered. These terms come from a region of integration in which the photon energy is of order  $m\alpha^2$ , which we refer to as the deep nonrelativistic region. One well-known complication associated with this region is that an infinite set of kernels contribute to order  $m\alpha^5$ . Here, however, we wish to discuss a second complication that is associated with the choice of bound-state formalism. To illustrate it, we first consider Eq. (21) when one photon is Coulomb and the other transverse. If we also make the change of variable  $k \rightarrow k+p$  this becomes

TABLE III. Contributions to the positronium hyperfine interval at order  $m\alpha^6$ .

Contribution	Coefficient of $m\alpha^6$
Derivative term	-0.04167
Many-potential term	0.42094
Two-photon exchange	-0.0227(30)
Three-photon exchange	-0.2861(17)
Total	0.0705(35)

$$\Delta E_{2\gamma X}(CT+TC) = 2ie^4 \int \frac{dk_0}{2\pi} \int \frac{d^3k}{(2\pi)^3} \int \frac{d^4p'}{(2\pi)^4} \int \frac{d^4p}{(2\pi)^4} \frac{1}{|\vec{p}' - \vec{p} - \vec{k}|^2} \left( \delta_{ij} - \frac{k_i k_j}{\vec{k}^2} \right) \\ \times \frac{\text{Tr}[\bar{\psi}(p') \gamma_0 (\not{P}/2 + \not{k} + \not{p} + m) \gamma_i \psi(p) \gamma_0 (-\not{P}/2 - \not{k} + \not{p}' + m) \gamma_j]}{[(P/2 + p + k)^2 - m^2 + i\epsilon][ (P/2 - p' + k)^2 - m^2 + i\epsilon][k^2 + i\epsilon]}. \quad (28)$$

If we close the contour above the real axis, only the pole  $k_0 = -|\vec{k}| \equiv -\omega$  contributes to order  $m\alpha^5$  in the deep nonrelativistic region. The denominator of the above expression then becomes

$$D = -2\omega[(W_0 + p_0 - \omega)^2 - |\vec{p} + \vec{k}|^2 - m^2] \\ \times [(W_0 - p'_0 - \omega)^2 - |\vec{p}' - \vec{k}|^2 - m^2]. \quad (29)$$

While in the present formalism  $p_0$  and  $p'_0$  vanish, we have kept them general in Eq. (29) for later comparison with the Barbieri-Remiddi formalism [15], in which they do not vanish. We can further simplify this denominator by neglecting  $\vec{k}$  with respect to  $\vec{p}$  and  $\vec{p}'$ , and  $\omega^2$  with respect to  $-2W_0\omega \approx -2m\omega$ . With these approximations, the denominator becomes, in the present formalism,

$$D \approx -2\omega(2m\omega + \vec{p}^2 + \gamma^2)(2m\omega + \vec{p}'^2 + \gamma^2). \quad (30)$$

However, suppose instead that we used the Barbieri-Remiddi formalism. In this formalism, the  $\delta$  function of  $p_0$  is replaced by

$$\delta(p_0) \rightarrow \frac{\omega_p - W_0}{-i\pi[p_0^2 - (\omega_p - W_0 - i\epsilon)^2]}, \quad (31)$$

with a similar replacement for  $\delta(p'_0)$ . While both formalisms emphasize the region  $p_0 = 0, p'_0 = 0$ , an extra integration must be carried out in the latter case. If we do this with Cauchy's theorem, the pole from the wave function gives  $p_0 = W_0 - \omega_p \approx -(\vec{p}^2 + \gamma^2)/2m$  and  $p'_0 \approx -(\vec{p}'^2 + \gamma^2)/2m$ . In the Barbieri-Remiddi formalism, the denominators then take the quite different form

$$D \approx -2\omega(2m\omega + 2\vec{p}^2 + 2\gamma^2)(2m\omega + 2\vec{p}'^2 + 2\gamma^2). \quad (32)$$

It is the latter form of the denominator that is encountered when the nonrelativistic Coulomb Green's function in the Bethe logarithm is expanded in terms of Coulomb potentials. This leads to the obvious question of how the Bethe logarithm arises in the present formalism. The basic problem is that, while considerable simplification is achieved by making the  $p_0$  dependence of the wave function a  $\delta$  function, forcing this dependence misses some deep nonrelativistic behavior in which  $p_0$  depends on  $(\vec{p}^2 + \gamma^2)/2m$ . This energy is of order

$m\alpha^2$ , so in situations in which the typical energy scale is of order  $m\alpha$ , as is the case for hyperfine splitting, there is little difference between the formalisms. However, when energies of order  $m\alpha^2$  are important, as in the Bethe logarithm, there is a difference and the Barbieri-Remiddi formalism includes the true behavior more naturally. Reintroduction of the correct low-energy behavior in the present formalism requires consideration of higher loop diagrams. In the present case, we have found that the *ctcy* diagram and the four-photon diagram of Fig. 6 play a role in reintroducing the correct behavior. In other words, these diagrams, which enter in order  $m\alpha^6$  and  $m\alpha^7$ , respectively, for hyperfine splitting, contribute at the unexpectedly low order of  $m\alpha^5$  for the singlet energy. This is an example of a case in which the  $R$  factor, even though it is designed to subtract out the leading behavior, can still contribute to a relatively low order.

At present, we are analyzing whether the awkward treatment of  $m\alpha^5$  terms present in our formalism can affect the order of interest for singlet and triplet states. The question is whether higher-order diagrams such as Fig. 4, after their leading  $m\alpha^5$  behavior is subtracted out, behave as  $m\alpha^6$  or  $m\alpha^7$ . In the latter case, the present method can be extended to singlet and triplet calculations, but in the former case either extra diagrams will have to be included or a formalism like that of Barbieri and Remiddi, with its more complicated structure, adopted. However, we stress that these issues involve only the singlet and triplet states individually, as the deep nonrelativistic region plays no role in hyperfine splitting to order  $m\alpha^6$ .

### III. COMPARISON WITH OTHER CALCULATIONS AND EXPERIMENT

As mentioned in the Introduction, two previous calculations of three-photon exchange have been carried out with differing results. The first calculation, in which NRQED was introduced [9], found the result

$$E_{3\gamma} = [-\frac{1}{6} \ln \alpha + 0.167(33)] m\alpha^6 \quad (33)$$

and the second, carried out in an effective Hamiltonian approach [10], obtained

$$E_{3\gamma} = [-\frac{1}{6} \ln \alpha + 0.3767(17)] m\alpha^6. \quad (34)$$

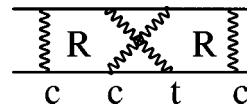


FIG. 6. Four-photon diagram contributing to singlet energies in order  $m\alpha^5$ .

The result of the present calculation is

$$E_{3\gamma} = \left[ -\frac{1}{6} \ln \alpha + 0.0705(35) \right] m\alpha^6. \quad (35)$$

The constant terms, using  $m\alpha^6 = 18.658$  MHz, are 3.12(0.66) MHz, 7.03(3) MHz, and 1.32(7) MHz. It was hoped that carrying out a third calculation would resolve the previous discrepancy, but this clearly is not the case. If the quoted NRQED error of  $0.033m\alpha^6$  is taken as a standard deviation, there is only a 0.2% chance of agreement. The present calculation is in unambiguous disagreement with the result of Ref. [10]. Unfortunately, it is not possible to compare the present calculation with either of the other approaches, as there is not a diagram-to-diagram correspondence. However, a recalculation in the NRQED framework is presently being carried out [21] and may shed light on this confusing situation.

There is a set of other contributions of order  $m\alpha^6$  that must be included before a comparison with experiment is made. Fortunately, they have all been carried out (see Table IV). Given the theoretical uncertainty of the three-photon exchange terms, it is useful to go through the status of the various terms with respect to their reliability. Beginning with three-photon annihilation, we note that a change from the original calculation of Cung *et al.* [22], which was, however, numerically very small, was found by Adkins *et al.* [23]. This was confirmed in a subsequent publication by Devoto and Repko [24]. A larger discrepancy was found for the one-loop radiative corrections to the two-photon-annihilation diagram [25,26]. However, it was shown that if certain errors were corrected in the earlier Feynman gauge calculation, precise agreement with the newer calculation, which was carried out in Fried-Yennie gauge, was found. Thus the same result for this term has effectively been found using two different gauges and it can be considered reliable. As mentioned above, two entirely independent calculations have given the same result for one-photon annihilation, so that can be taken as certain. This is also the case for the fourth row of Table IV, which arises simply from the well-known one- and two-loop  $g-2$  factors. Finally, radiative recoil calculations have also been calculated with two different approaches [11,12]. In this case there is a slight discrepancy of 0.1 MHz, which, while well under the experimental uncertainty, should be understood. Present computer power should allow a reduction of the numerical error quoted in the earlier work: this is under present investigation.

The present status of the  $m\alpha^6$  constant terms is summarized in Table IV. If this is combined with the lower-order terms,

$$\Delta\nu = m\alpha^4 \left[ \frac{7}{12} - \frac{\alpha}{\pi} \left( \frac{8}{9} + \frac{1}{2} \ln 2 \right) - \frac{5}{24} \alpha^2 \ln \alpha \right], \quad (36)$$

which give 203 400.29 MHz, our result is

$$\Delta\nu = 203\,387.26(7)\text{MHz}. \quad (37)$$

Using instead the Caswell-Lepage result gives 203 389.06(62) MHz and the effective Hamiltonian result of Pachucki gives 203 392.97(3) MHz.

The two experimental values of highest precision are those of Mills and Bearman [28], who found

TABLE IV. Contributions to the positronium hyperfine interval at order  $m\alpha^6$ .

Contribution	$K$	$\Delta E$ (MHz)
Three-photon annihilation <sup>a</sup>	-0.05194	-0.969
Two-photon annihilation <sup>b</sup>	-0.03248	-0.606
One-photon annihilation <sup>c</sup>	-0.12565	-2.344
$O(\alpha^2)$ corrections to one-photon exchange <sup>d</sup>	-0.01374	-0.256
Radiative recoil <sup>e</sup>	-0.5453	-10.17
Present calculation	0.0705(35)	1.32(7)
Total	-0.6986(35)	-13.03(7)

<sup>a</sup>References [22–24].

<sup>b</sup>References [25, 26].

<sup>c</sup>References [7, 8].

<sup>d</sup>Reference [27].

<sup>e</sup>References [11, 12].

$$\Delta\nu = 203\,387.5(1.6)\text{MHz}, \quad (38)$$

and Ritter *et al.* [29], who determined

$$\Delta\nu = 203\,389.10(0.74)\text{MHz}. \quad (39)$$

The Mills-Bearman experiment is consistent with both our result and the Caswell-Lepage result, while the more accurate Ritter *et al.* experiment is mildly discrepant with the present calculation and consistent with that of Caswell and Lepage. Both experiments are in strong disagreement with the effective Hamiltonian calculation. An additional theoretical issue is the size of uncalculated  $m\alpha^7$  terms. One such term, involving a factor of  $\ln^2 \alpha$ , has been calculated by Karshenboim [30] and contributes  $-0.92$  MHz. We have not included it in our analysis because of the unknown size of the nonleading terms. In fact, a recent calculation of part of the two-loop Lamb shift [31], in which a complete calculation was compared with the leading logarithm term, also calculated by Karshenboim [30], provides an example of a case in which the nonleading corrections are apparently larger than the leading logarithm. Thus, until a complete calculation of all  $m\alpha^7$  terms is carried out, it seems to us most advisable simply to note that they can enter at the 1-MHz level, which we take as the level of theoretical uncertainty. While such a calculation presents a significant long-range challenge to bound-state QED theory, by far the most pressing present theoretical issue for ground-state positronium hyperfine splitting is the resolution of the now three-way discrepancy in the recoil calculation.

#### ACKNOWLEDGMENTS

The work of J.S. was partially supported by NIST under precision measurement Grant No. 60NANB6D0036 and that of G.A. by the NSF under Grants Nos. PHY-9711991 and PHY-9722074. We would like to thank D. Fell, D. Gidley, G. P. Lepage, and K. Pachucki for useful conversations.



- [1] J. Pirenne, Arch. Sci. Phys. Nat. **29**, 265 (1947).
- [2] V. B. Berestetski and L. D. Landau, Zh. Eksp. Teor. Fiz. **19**, 673 (1949).
- [3] R. A. Ferrell, Phys. Rev. **84**, 858 (1951).
- [4] T. Fulton and P. Martin, Phys. Rev. **95**, 811 (1954).
- [5] G. P. Lepage, Phys. Rev. A **16**, 863 (1977); G. T. Bodwin and D. R. Yennie, Phys. Rep., Phys. Lett. **43C**, 267 (1978).
- [6] R. N. Fell, Phys. Rev. Lett. **68**, 25 (1992); I. B. Khriplovich, A. I. Milstein, and A. S. Yelkhovskiy, Phys. Lett. B **282**, 237 (1992); R. N. Fell, I. B. Khriplovich, A. I. Milstein, and A. S. Yelkhovskiy, Phys. Lett. A **181**, 172 (1993).
- [7] G. S. Adkins, R. N. Fell, and P. M. Mitrikov, Phys. Rev. Lett. **79**, 3383 (1997).
- [8] A. H. Hoang, P. Labelle, and S. M. Zebarjad, Phys. Rev. Lett. **79**, 3387 (1997).
- [9] W. E. Caswell and G. P. Lepage, Phys. Lett. **167B**, 437 (1986).
- [10] K. Pachucki, Phys. Rev. A **56**, 297 (1997).
- [11] J. R. Sapirstein, E. A. Terray, and D. R. Yennie, Phys. Rev. D **29**, 2290 (1984).
- [12] K. Pachucki and S. G. Karshenboim, Phys. Rev. Lett. **80**, 2101 (1998).
- [13] W. E. Caswell and G. P. Lepage, Phys. Rev. A **18**, 810 (1978).
- [14] G. S. Adkins and R. N. Fell (unpublished).
- [15] R. Barbieri and E. Remiddi, Nucl. Phys. B **141**, 413 (1978).
- [16] G. P. Lepage, J. Comput. Phys. **27**, 192 (1978).
- [17] R. Karplus and A. Klein, Phys. Rev. **87**, 848 (1952).
- [18] R. N. Fell, Ph.D. thesis, Brandeis University, 1990 (unpublished).
- [19] G. P. Lepage, Phys. Rev. A **16**, 863 (1977).
- [20] For the sums  $ctcy+ccty+tccz$  and  $ctt0+ttc0+ctty$  we found 0.0536(9) and  $-0.1272(8)$ , respectively, as the coefficients of  $m\alpha^6$ .
- [21] G. P. Lepage (private communication).
- [22] V. K. Cung, A. Devoto, T. Fulton, and W. W. Repko, Phys. Lett. **68B**, 474 (1977); Nuovo Cimento A **43**, 643 (1978).
- [23] G. S. Adkins, M. H. T. Bui, and D. Zhu, Phys. Rev. A **37**, 4071 (1988).
- [24] A. Devoto and W. W. Repko, Phys. Rev. A **42**, 5730 (1990).
- [25] V. K. Cung, A. Devoto, T. Fulton, and W. W. Repko, Phys. Lett. **78B**, 116 (1978); Phys. Rev. A **19**, 1886 (1979).
- [26] G. S. Adkins, Y. M. Aksu, and M. H. T. Bui, Phys. Rev. A **47**, 2640 (1993).
- [27] The only one-photon-exchange contributions come from the electron and positron anomalous moments:  $m\alpha^4/3$  times the  $O(\alpha^2)$  part of  $(1+a_e)^2$ .
- [28] A. P. Mills, Jr., Phys. Rev. A **27**, 262 (1983): This corrects the measurement of A. P. Mills, Jr. and G. H. Bearman, Phys. Rev. Lett. **34**, 246 (1975).
- [29] M. W. Ritter, P. O. Egan, V. W. Hughes, and K. A. Woodle, Phys. Rev. A **30**, 1331 (1984).
- [30] S. Karshenboim, JETP **76**, 541 (1993).
- [31] S. Mallampalli and J. Sapirstein, Phys. Rev. Lett. **80**, 5297 (1998).